Other Extensions of the k-ε Model

Another extension of the k-ε model was developed by Yakhot et al. With techniques from renormalization group theory they proposed the so-called RNG k-ε model

$$u\frac{\partial k}{\partial x} + v\frac{\partial k}{\partial y} = \frac{\partial}{\partial y}\left(\frac{\varepsilon_m}{\sigma_k}\frac{\partial k}{\partial y}\right) + \varepsilon_m\left(\frac{\partial u}{\partial y}\right)^2 - \varepsilon$$

$$u\frac{\partial \varepsilon}{\partial x} + v\frac{\partial \varepsilon}{\partial y} = \frac{\partial}{\partial y}\left(\frac{\varepsilon_m}{\sigma_\varepsilon}\frac{\partial \varepsilon}{\partial y}\right) + c_{\varepsilon 1}\frac{\varepsilon}{k}\varepsilon_m\left(\frac{\partial u}{\partial y}\right)^2 - c_{\varepsilon 2}\frac{\varepsilon^2}{k}$$

$$c_{\varepsilon 1} = 1.42, \qquad c_{\varepsilon 2} = 1.68 + \frac{c_\mu \lambda^3(1 - \lambda/\lambda_0)}{1 + 0.012\lambda^3}$$

$$\lambda = \frac{k}{\varepsilon}\sqrt{2s_{ij}s_{ji}}, \qquad \lambda_0 = 4.38, \qquad c_\mu = 0.085$$

$$\sigma_k = 0.72, \qquad \sigma_\varepsilon = 0.72, \qquad s_{ij} = \frac{1}{2}\left(\frac{\partial u_i}{\partial x_j} + \frac{\partial u_j}{\partial x_i}\right)$$

Wilcox k-ω Model

$$\varepsilon_m = \frac{k}{\omega}$$

the turbulence kinetic energy and specific dissipation rate equations are

$$\frac{Dk}{Dt} = \frac{\partial}{\partial x_k}\left[\left(\nu + \frac{\varepsilon_m}{\sigma_k}\right)\frac{\partial k}{\partial x_k}\right] + R_{ik}\frac{\partial \overline{u}_i}{\partial x_k} - \beta^* k\omega$$

$$\frac{D\omega}{Dt} = \frac{\partial}{\partial x_k}\left[\left(\nu + \frac{\varepsilon_m}{\sigma_\omega}\right)\frac{\partial \omega}{\partial x_k}\right] + \alpha\frac{\omega}{k}R_{ik}\frac{\partial \overline{u}_i}{\partial x_k} - \beta\omega^2$$

$$R_{ij} = \varepsilon_m\left(\frac{\partial \overline{u}_i}{\partial x_j} + \frac{\partial \overline{u}_j}{\partial x_i}\right) \qquad \alpha = \frac{13}{25}, \quad \beta = \beta_0 f_\beta, \quad \beta^* = \beta_0^* f_\beta, \quad \sigma_k = 2, \quad \sigma_\omega = 2$$

$$\beta_0 = \frac{9}{125}, \quad f_\beta = \frac{1 + 70\chi_\omega}{1 + 80\chi_\omega}, \quad \chi_\omega = \left|\frac{\Omega_{ij}\Omega_{jk}S_{ki}}{(\beta_0^*\omega)^3}\right| \qquad\qquad \Omega_{ij} = \frac{1}{2}\left(\frac{\partial \overline{u}_i}{\partial x_j} - \frac{\partial \overline{u}_j}{\partial x_i}\right)$$

Mean rotation tensor

$$\beta_0^* = \frac{9}{100}, \quad f_\beta = \begin{cases} 1, & \chi_k \leq 0 \\ \dfrac{1 + 680\chi_k^2}{1 + 400\chi_k^2}, & \chi_k > 0 \end{cases}, \quad \chi_k = \frac{1}{\omega^3}\frac{\partial k}{\partial x_j}\frac{\partial \omega}{\partial x_j} \qquad S_{ki} = \frac{1}{2}\left(\frac{\partial \overline{u}_k}{\partial x_i} + \frac{\partial \overline{u}_i}{\partial x_k}\right)$$

mean-strain-rate tensors

The parameter χ_ω is zero for two-dimensional flows

$\boxed{l = \dfrac{\sqrt{k}}{\omega}}$ ⟹ length scale in the eddy viscosity

$\boxed{\varepsilon = \beta^*\omega k}$ ⟹ dissipation

Non-linear Eddy-viscosity Models

$\overline{u_i u_j}$ is formulated from the Boussinesq assumption

$$a_{ij} = -2\nu_t \frac{\bar{S}_{ij}}{k} \qquad \text{where the anisotropy tensor is defined as} \qquad \boxed{a_{ij} \equiv \frac{\overline{u_i u_j}}{k} - \frac{2}{3}\delta_{ij}}$$

$$\bar{S}_{ij} = \frac{1}{2}\left(\frac{\partial \bar{U}_i}{\partial x_j} + \frac{\partial \bar{U}_j}{\partial x_i}\right)$$

The relation between the stress $\overline{u_i u_j}$ and the velocity gradient is, as can be seen, linear.

The nonlinear relation form is

$$a_{ij} = -2c_\mu \tau \bar{S}_{ij}$$

$$+ c_1 \tau^2 \left(\bar{S}_{ik}\bar{S}_{kj} - \frac{1}{3}\bar{S}_{\ell k}\bar{S}_{\ell k}\delta_{ij}\right) + c_2 \tau^2 \left(\bar{\Omega}_{ik}\bar{S}_{kj} + \bar{\Omega}_{jk}\bar{S}_{ki}\right)$$

$$+ c_3 \tau^2 \left(\bar{\Omega}_{ik}\bar{\Omega}_{jk} - \frac{1}{3}\bar{\Omega}_{\ell k}\bar{\Omega}_{\ell k}\delta_{ij}\right) + c_4 \tau^3 \left(\bar{S}_{ki}\bar{\Omega}_{\ell j} + \bar{\Omega}_{\ell i}\bar{S}_{kj}\right)\bar{S}_{k\ell}$$

$$+ c_5 \tau^3 \left(\bar{\Omega}_{i\ell}\bar{\Omega}_{\ell m}\bar{S}_{mj} + \bar{S}_{i\ell}\bar{\Omega}_{\ell m}\bar{\Omega}_{mj} - \frac{2}{3}\bar{\Omega}_{mn}\bar{S}_{\ell m}\bar{\Omega}_{n\ell}\delta_{ij}\right)$$

$$+ c_6 \tau^3 \bar{S}_{k\ell}\bar{S}_{k\ell}\bar{S}_{ij} + c_7 \tau^3 \bar{\Omega}_{k\ell}\bar{\Omega}_{k\ell}\bar{S}_{ij}$$

τ is a turbulent time scale and for a non-linear $k - \varepsilon$ model $\tau = k/\varepsilon$, and for a non-linear $k - \omega$ model $\tau = 1/\omega$

However, note that it is only quadratic in $\bar{S}_{ij}$ and Ω_{ij}.
This is due to Cayley-Hamilton theorem which states that a tensor is only linearly independent up to quadratic terms; this means that

for example, $\bar{S}_{ij}^3 = \bar{S}_{ik}\bar{S}_{kl}\bar{S}_{lj}$ can be expressed as a linear combination of $\bar{S}_{ij}^2 = \bar{S}_{ik}\bar{S}_{kj}$ and $\bar{S}_{ij}$.

a_{ij} is symmetric and its trace is zero; it is easily verified that the right-hand side of Eq. 48 also has these properties. Examples of non-linear models (sometimes also called *explicit* algebraic stress models) in the literature are the models of Gatski & Speziale (1993), Shih *et al.* (1995), Craft *et al.* (1997) and Wallin & Johansson (2000).

in fully developed channel flow ($\bar{U}_2 = \bar{U}_3 = \partial/\partial x_1 = \partial/\partial x_3 \equiv 0$); we obtain

$$a_{11} = \frac{1}{12}\tau^2 \left(\frac{\partial \bar{U}_1}{\partial x_2}\right)^2 (c_1 + 6c_2 + c_3) \qquad a_{33} = -\frac{1}{6}\tau^2 \left(\frac{\partial \bar{U}_1}{\partial x_2}\right)^2 (c_1 + c_3)$$

$$a_{22} = \frac{1}{12}\tau^2 \left(\frac{\partial \bar{U}_1}{\partial x_2}\right)^2 (c_1 - 6c_2 + c_3) \qquad a_{12} = -c_\mu \tau \frac{\partial \bar{U}_1}{\partial x_2} + \frac{1}{4}\tau^3 \left(\frac{\partial \bar{U}_1}{\partial x_2}\right)^3 (-c_5 + c_6 + c_7)$$

For constants as in Craft *et al.* (1997), i.e $c_1 = -0.05$, $c_2 = 0.11$, $c_3 = 0.21$, $c_4 = -0.8$ $c_5 = 0$, $c_6 = -0.5$ and $c_7 = 0.5$ we get

$$a_{ij} \equiv \frac{\overline{u_i u_j}}{k} - \frac{2}{3}\delta_{ij}$$

$$a_{11} = \frac{0.82}{12}\tau^2\left(\frac{\partial \bar{U}_1}{\partial x_2}\right)^2 \Rightarrow \overline{u_1^2} = \frac{2}{3}k + \frac{0.82}{12}k\tau^2\left(\frac{\partial \bar{U}_1}{\partial x_2}\right)^2$$

$$a_{22} = \frac{-0.5}{12}\tau^2\left(\frac{\partial \bar{U}_1}{\partial x_2}\right)^2 \Rightarrow \overline{u_2^2} = \frac{2}{3}k - \frac{0.5}{12}k\tau^2\left(\frac{\partial \bar{U}_1}{\partial x_2}\right)^2$$

$$a_{33} = \frac{-0.16}{12}\tau^2\left(\frac{\partial \bar{U}_1}{\partial x_2}\right)^2 \Rightarrow \overline{u_3^2} = \frac{2}{3}k - \frac{0.16k}{12}\tau^2\left(\frac{\partial \bar{U}_1}{\partial x_2}\right)^2$$

$$a_{12} = -c_\mu\frac{k}{\varepsilon}\frac{\partial \bar{U}_1}{\partial x_2}$$

We find that indeed the non-linear model gives anisotropic normal Reynolds stresses.

streamline curvature effects ⟹ effect of secondary strains such as $\partial \bar{U}_2 / \partial x_1$

$$a_{11} = \frac{1}{12}\tau^2 \left(\frac{\partial \bar{U}_2}{\partial x_1}\right)^2 (c_1 - 6c_2 + c_3)$$

$$a_{22} = \frac{1}{12}\tau^2 \left(\frac{\partial \bar{U}_2}{\partial x_1}\right)^2 (c_1 + 6c_2 + c_3)$$

$$a_{33} = -\frac{1}{6}\tau^2 \left(\frac{\partial \bar{U}_2}{\partial x_1}\right)^2 (c_1 + c_3)$$

$$a_{12} = -\frac{1}{4}\tau^3 \left(\frac{\partial \bar{U}_2}{\partial x_1}\right)^3 (c_5 + c_6 + c_7)$$

⟹

$$a_{11} = -\frac{0.5}{12}\tau^2 \left(\frac{\partial \bar{U}_2}{\partial x_1}\right)^2$$

$$a_{22} = \frac{0.82}{12}\tau^2 \left(\frac{\partial \bar{U}_2}{\partial x_1}\right)^2$$

$$a_{33} = -\frac{0.16}{12}\tau^2 \left(\frac{\partial \bar{U}_2}{\partial x_1}\right)^2, \quad a_{12} = 0$$

$$a_{12} = -2\left[c_\mu + \frac{1}{4}(c_7 - c_5)\left(S^2 - \Omega^2\right)\right]\frac{k}{\varepsilon}S_{12}$$

$$S = \frac{k}{\varepsilon}\sqrt{2S_{ij}S_{ij}}, \qquad \Omega = \frac{k}{\varepsilon}\sqrt{2\Omega_{ij}\Omega_{ij}}$$

if $c_7 - c_5$ is chosen positive

the shear stress will increase when $S^2 - \Omega^2 > 0$ and will decrease when $S^2 - \Omega^2 < 0$.
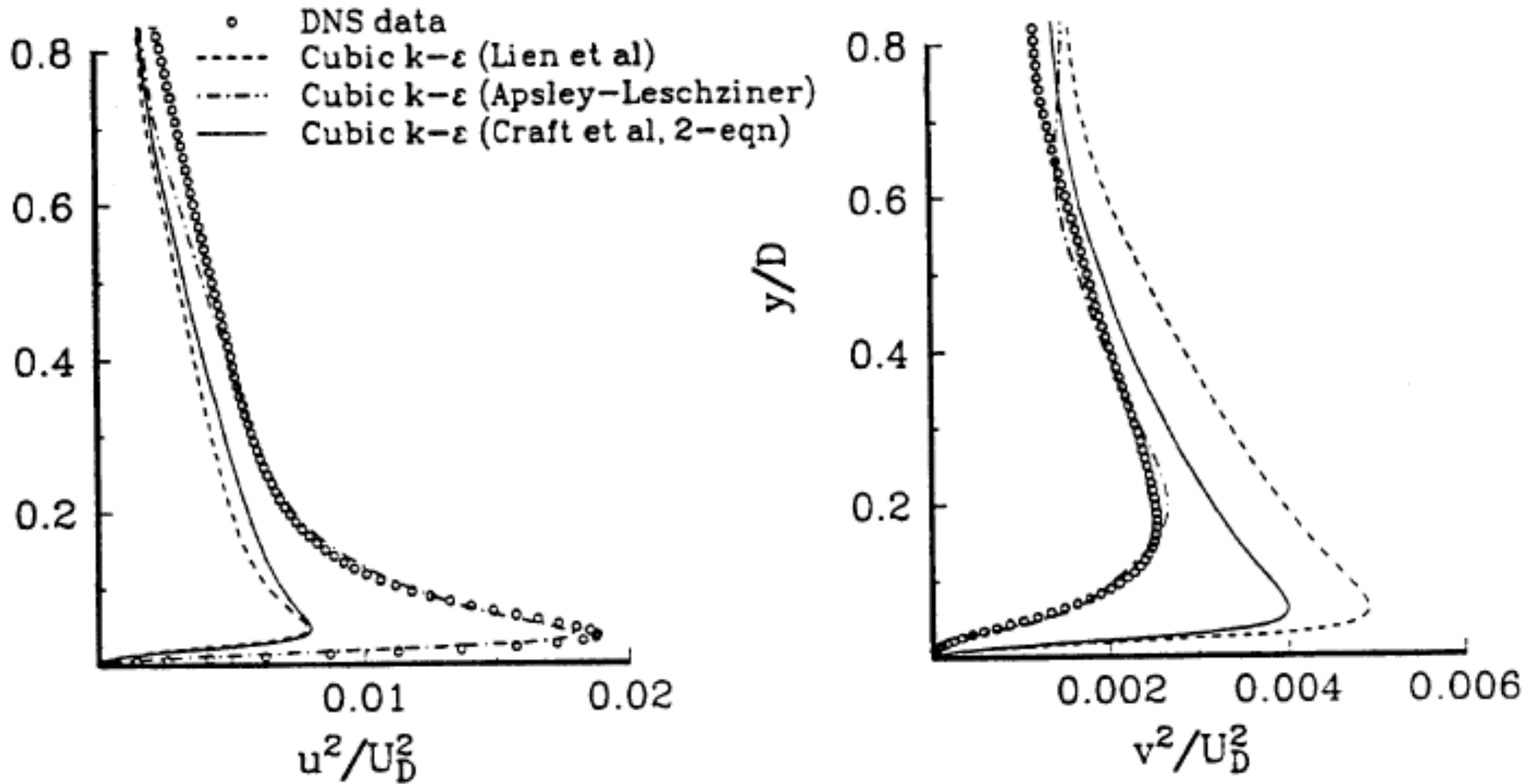
Apsley and Leschziner

Fig. 17. Normal-stress distributions in fully-developed channel flow at $Re = 7890$ predicted by different non-linear EVMs (Apsley and Leschziner [107]).

Ref. New Trends in Turbulence, 2000

Cost and ease of use

In this discussion we take the k–ε model as a reference: the model is incorporated into most commercial CFD codes, and it is generally regarded as being easy to use and computationally inexpensive when it is used in conjunction with wall functions.

If wall functions are not employed, the task of performing k–ε calculations for the viscous near-wall region is significantly more difficult and expensive. This is due to the need to resolve k and ε (which vary strongly in the near-wall region); and also to the fact that the source terms in these equations become very large close to the wall. (In the log-law region, the term $C_{\varepsilon2}\varepsilon^2/k$ varies as u_τ^4/y^2.)

The Spalart–Allmaras model is – by design – much simpler and less expensive for near-wall aerodynamic flows. This is because, compared with k and ε, the turbulent viscosity ν_T behaves benignly in the near-wall region, and is more easily resolved.

In comparison with the k–ε model, Reynolds-stress models are somewhat more difficult and costly because

(i) in general there are seven turbulence equations to be solved (for $\langle u_i u_j \rangle$ and ε) instead of two (for k and ε);

(ii) the model Reynolds-stress equation is substantially more complicated than the k equation (and hence requires coding effort); and

(iii) in the mean-momentum equation, the term

$$-\frac{\partial}{\partial x_i}\langle u_i u_j \rangle$$

results in a less favorable numerical coupling between the flow and turbulence equations than does the corresponding term

$$\frac{\partial}{\partial x_i}\left[v_{\mathrm{T}}\left(\frac{\partial \langle U_i \rangle}{\partial x_j} + \frac{\partial \langle U_j \rangle}{\partial x_i} \right) \right] \quad \text{in the } k\text{–}\varepsilon \text{ model.}$$

Typically, the CPU time required for a Reynolds-stress-model calculation can be more than that for a $k-\varepsilon$ calculation by a factor of two.

The primary motivation for the use of algebraic stress models is to avoid the cost and difficulty of solving the Reynolds-stress model equations. However, the general experience is that these benefits are not realized. The algebraic stress model equations are coupled nonlinear equations, often with multiple roots, which are non-trivial to solve economically. In addition, with respect to item (iii) above, algebraic stress models have the same disadvantage as Reynolds-stress models. As discussed in the previous section, algebraic stress models can be recast as nonlinear viscosity models. These add little cost and difficulty to $k-\varepsilon$-model calculations.

Range of applicability

The basic k–ε and Reynolds-stress models can be applied to any turbulent flow. They also provide lengthscale and timescale information that can be used in the modelling of additional processes. Consequently, they provide a basis for the modelling of turbulent reactive flows, multi-phase flows, etc. Model transport equations for the scalar flux can be solved in conjunction with a Reynolds-stress model to provide closure to the mean scalar equations. Such so-called *second-moment closures* have successfully been extended to atmospheric flows in which buoyancy effects are significant (e.g., Zeman and Lumley (1976)). Although it can, in principle, be applied to any turbulent flow (in the class considered), the Spalart–Allmaras model is intended only for aerodynamic applications.

Accuracy

(i) The k–ε model performs reasonably well for two-dimensional thin shear flows in which the mean streamline curvature and mean pressure gradient are small.

(ii) For boundary layers with strong pressure gradients the k–ε model performs poorly. However, the k–ω model performs satisfactorily, and indeed its performance is superior for many flows.

(iii) For flows far removed from simple shear (e.g., the impinging jet and three-dimensional flows), the k–ε model can fail profoundly.

(iv) The use of nonlinear viscosity models is beneficial and allows the calculation of secondary flows (which cannot be calculated using the isotropic viscosity hypothesis).

(v) Reynolds-stress models can be successful (whereas turbulent viscosity models are not) in calculating flows with significant mean streamline curvature, flows with strong swirl or mean rotation, secondary flows in ducts, and flows with rapid variations in the mean flow.

(vi) Reynolds-stress-model calculations are sensitive to the details of the modelling of the pressure–rate-of-strain tensor, including wall-reflection terms.

(vii) The elliptic relaxation models (both Reynolds-stress and k–ε–$\overline{v^2}$) have been quite successful in application to a number of challenging two-dimensional flows, including the impinging jet, and separated boundary layers.

(viii) The dissipation equation is frequently blamed for poor performance of a model. For many flows, much improved performance can be obtained by altering the model constants ($C_{\varepsilon 1}$ or $C_{\varepsilon 2}$) or by adding correction terms. No correction to the dissipation equation that is effective in all flows has been found.

> *In summary, especially for complex flows, Reynolds-stress models have been demonstrated to be superior to two-equation models.*

the ratio between the characteristic length of the most energetic scale, L, and that of the smallest dynamically active scale, η, is evaluated by the relation

$$\frac{L}{\eta} = O\left(Re^{3/4}\right)$$

$O\left(Re^{9/4}\right)$ degrees of freedom in order to be able to represent all the scales in

The ratio of characteristic times varies as $O\left(Re^{1/2}\right)$

but the use of explicit time-integration algorithm leads to a linear dependency of the time step with respect to the mesh size

we have to solve the Navier–Stokes equations numerically $O\left(Re^{3}\right)$ times

Usual Levels of Approximation

By calculating the statistical average of the solution directly. This is called the Reynolds Averaged Numerical Simulation (RANS), which is used mostly for engineering calculations. The exact solution *u* splits into the sum of its statistical average *<u>* and a fluctuation *u'* (see Appendix A):

$$u(x,t) = \langle u(x,t) \rangle + u'(x,t)$$

$$\langle u(x,t) \rangle \approx \overline{u}(x) = \lim_{T \to \infty} \frac{1}{T} \int_0^T u(x,t) dt$$

This splitting, or "decomposition", is illustrated below. The fluctuation *u'* is not represented directly by the numerical simulation, and is included only by way of a turbulence model.

TOTAL = RESOLVED + MODELED
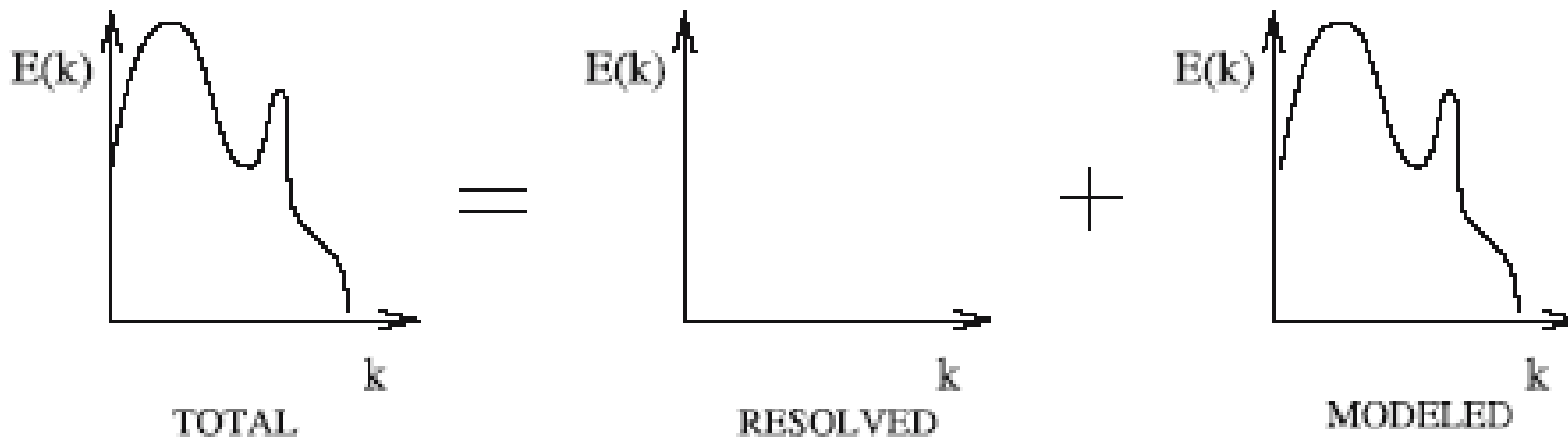
By calculating directly only certain low-frequency modes in time (of the order of a few hundred hertz) and the average field. This approach goes by a number of names: *Unsteady Reynolds Averaged Numerical Simulaton* (URANS), *Semi-Deterministic Simulation* (SDS), *Very Large-Eddy Simulation* (VLES), and sometimes *Coherent Structure Capturing* (CSC). The field **u** appears here as the sum of three contributing terms:

$$u(x,t) = \overline{u}(x) + \langle u(x,t) \rangle_c + u'(x,t)$$

The first term is the *time average of the exact solution*, the second its *conditional statistical average*, and the third the *turbulent fluctuation*.

TOTAL = RESOLVED + MODELED
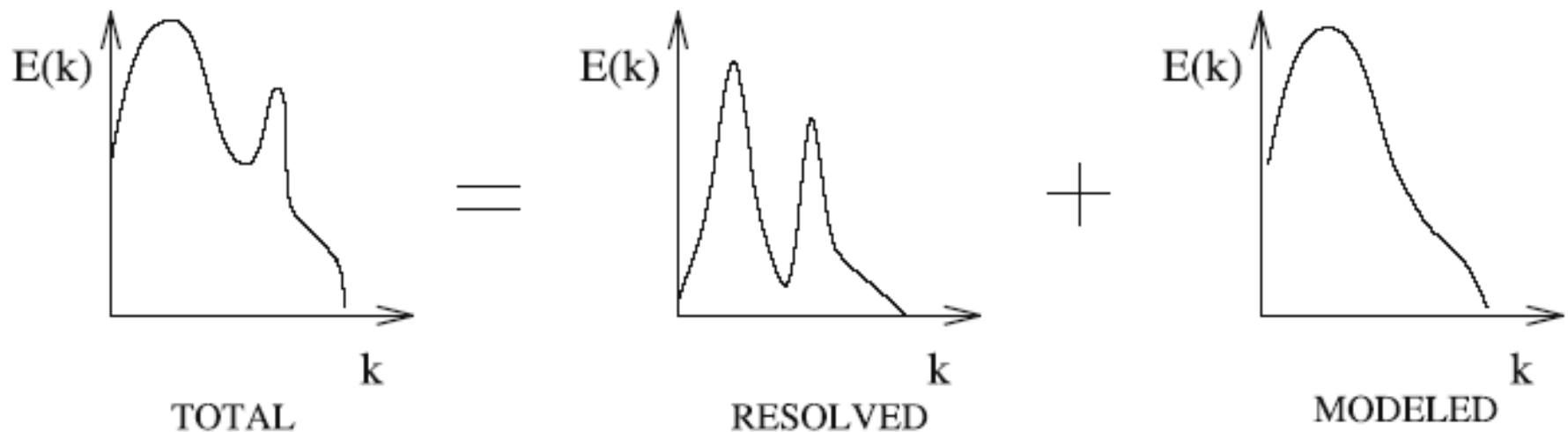
By calculating only the low-frequency modes in space directly. This is what is done in *Large-Eddy Simulation* (LES). It is this approach that is discussed in the following.
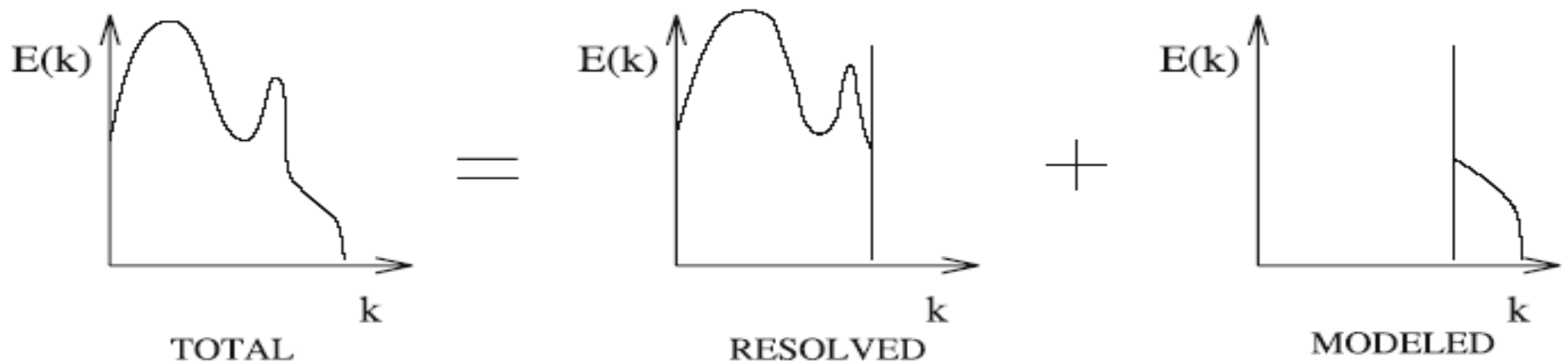
Decomposition of the energy spectrum in the solution associated with large eddy simulation (symbolic representation).
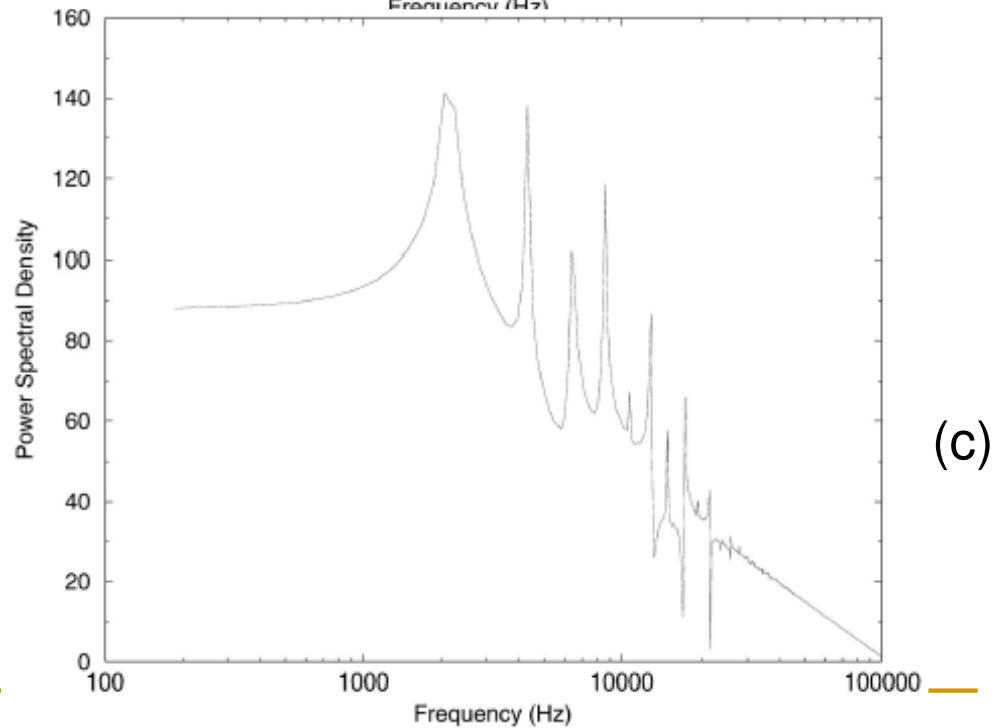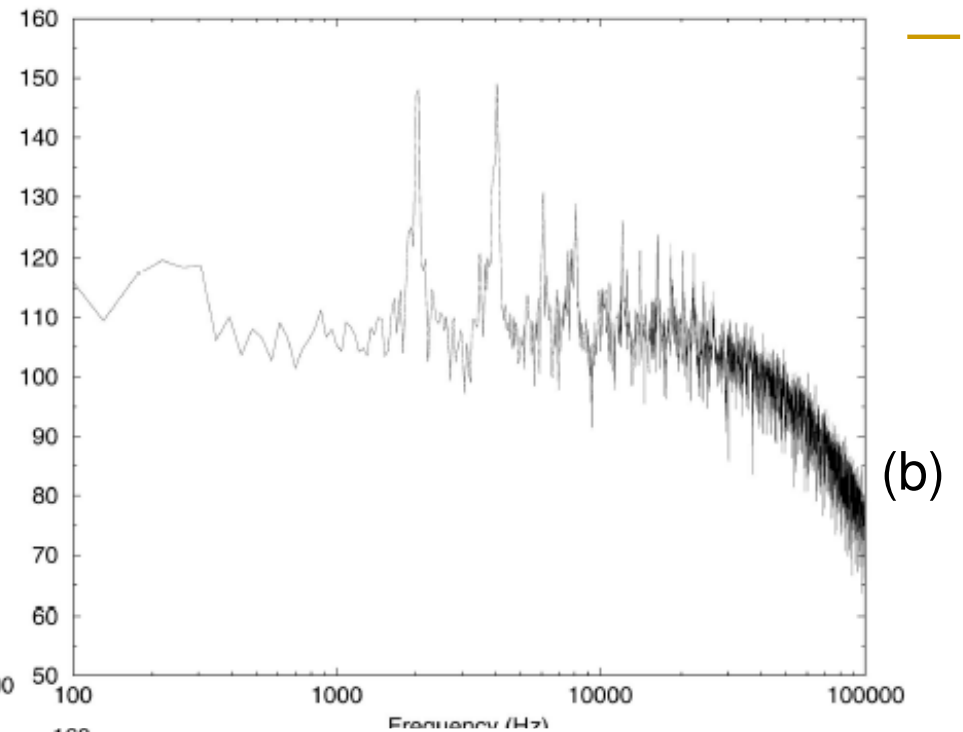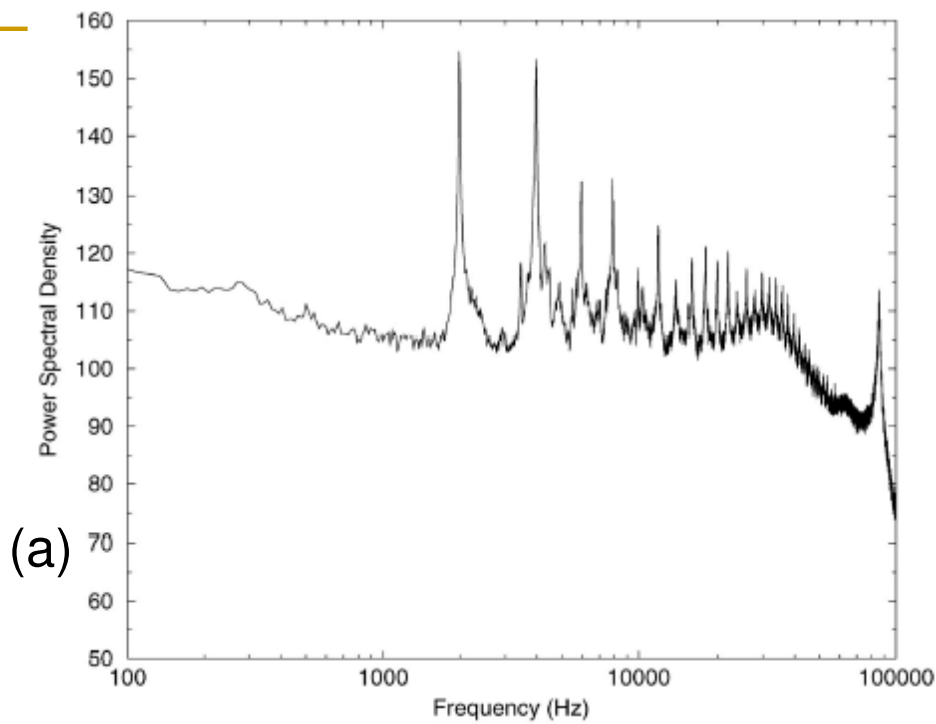
Pressure spectrum inside a cavity. (a) experimental data (ideal direct numerical simulation) (courtesy of L. Jacquin, ONERA); *(b)*: large-eddy simulation(Courtesy of L. Larchevêque, ONERA); *(c)*: unsteady RANS simulation (Courtesy of V. Gleize, ONERA).

resolved

subgrid

$\overline{\Delta}$

$k_c = \pi/\overline{\Delta}$

Log(E(k))

Log(k)
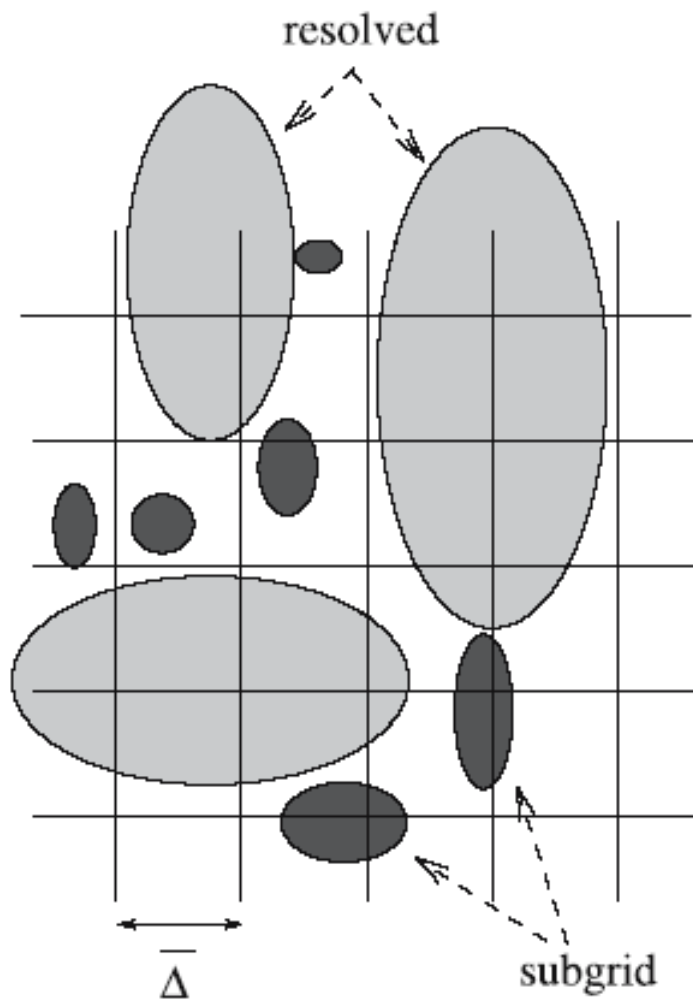
PHYSICAL SPACE
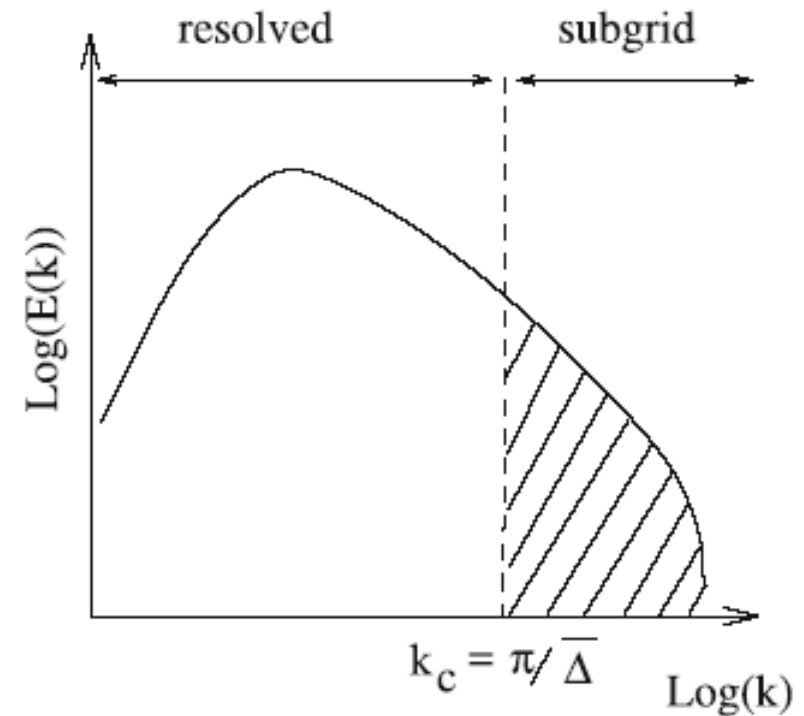
FOURIER SPACE

Fig. 1.5. Schematic view of the simplest scale separation operator: grid and theoretical filters are the same, yielding a sharp cutoff filtering in Fourier space between the resolved and subgrid scales. The associated cutoff wave number is denoted k_c, which is directly computed from the cutoff length $\overline{\Delta}$ in the physical space. Here, $\overline{\Delta}$ is assumed to be equal to the size of the computational mesh.
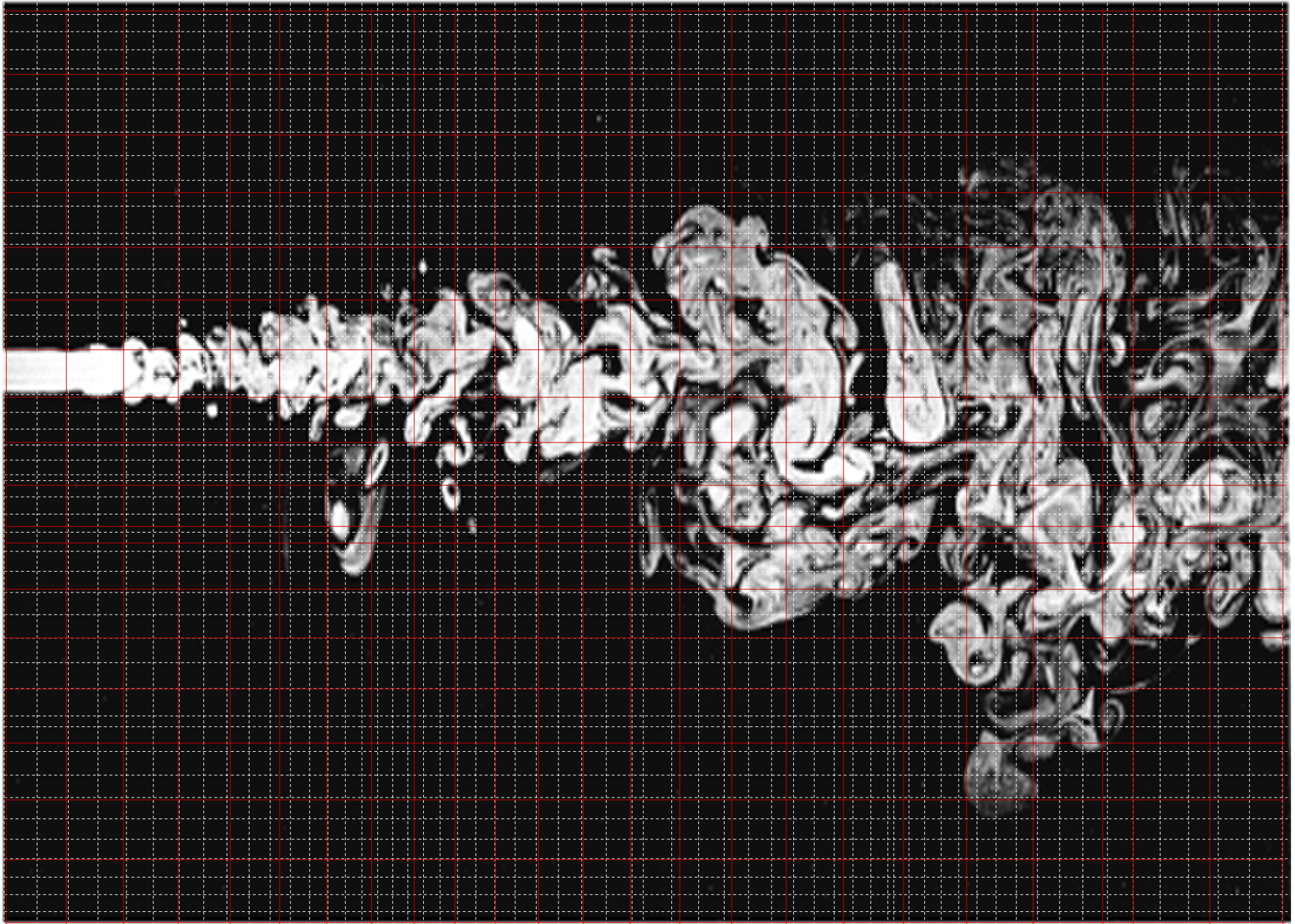
In LES we filter (volume average) the equations. In 1D we get:

$$\bar{\Phi}(x,t) = \frac{1}{\Delta x} \int_{x-0.5\Delta x}^{x+0.5\Delta x} \Phi(\xi,t)d\xi$$

$$\Phi = \bar{\Phi} + \Phi''$$
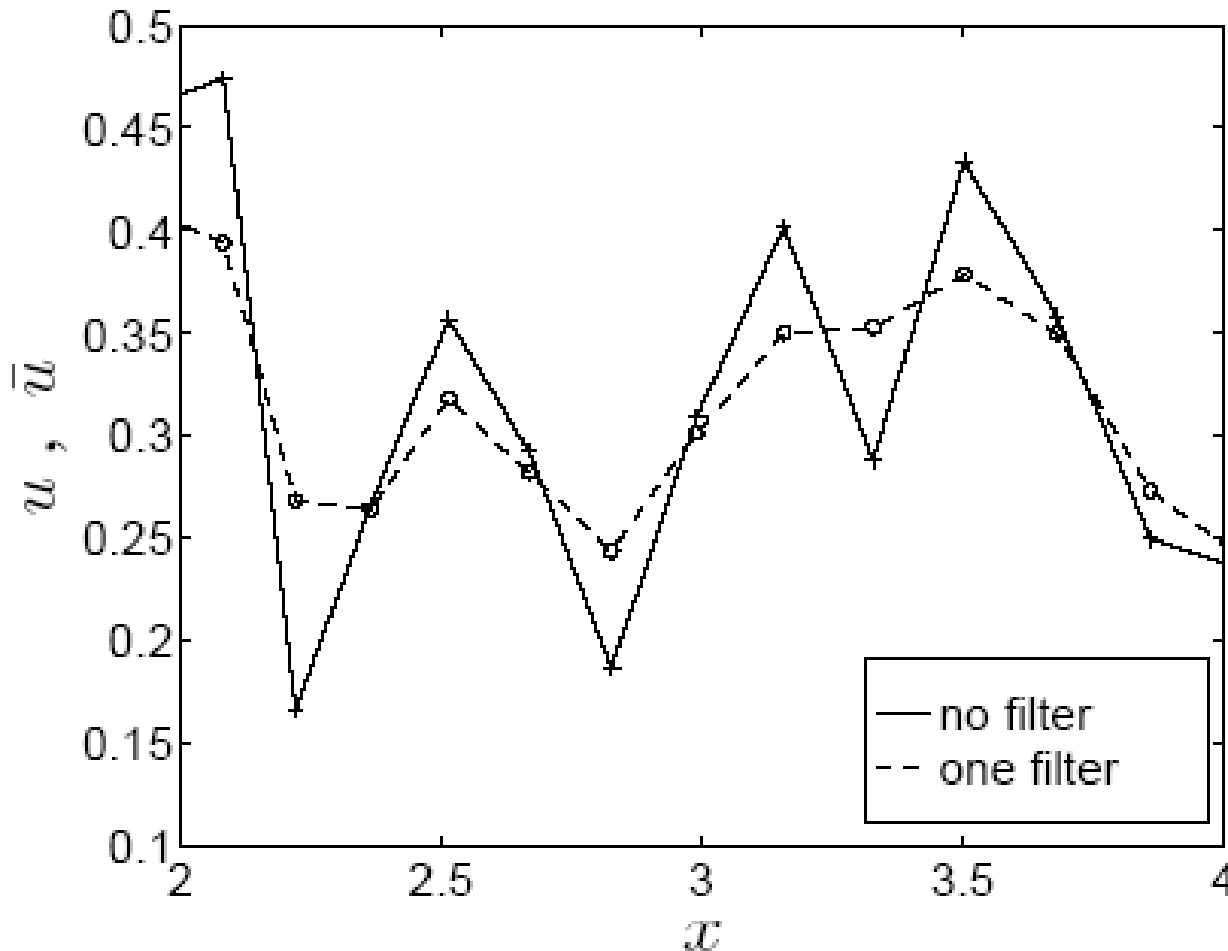
Since in LES we do not average in time, the filtered variables are functions of space and time.

In order to be able to manipulate the Navier–Stokes equations after applying a filter, we require that the filter verify the three following properties:

1. Conservation of constants

$$\bar{a} = a \Longleftrightarrow \int_{-\infty}^{+\infty} \int_{-\infty}^{+\infty} G(\xi, t') d^3\xi dt' = 1$$

2. Linearity

$$\overline{\phi + \psi} = \bar{\phi} + \bar{\psi}$$

3. Commutation with derivation

$$\overline{\frac{\partial \phi}{\partial s}} = \frac{\partial \bar{\phi}}{\partial s}, \quad s = x, t$$

Three Classical Filters for Large-Eddy Simulation

Three convolution filters are ordinarily used for performing the spatial scale separation. For a cutoff length $\overline{\Delta}$, in the mono-dimensional case, these are written:

Box or top-hat filter:

$$G(x - \xi) = \begin{cases} \dfrac{1}{\overline{\Delta}} & \text{if } |x - \xi| \le \dfrac{\overline{\Delta}}{2} \\ \\ 0 & \text{otherwise} \end{cases}$$
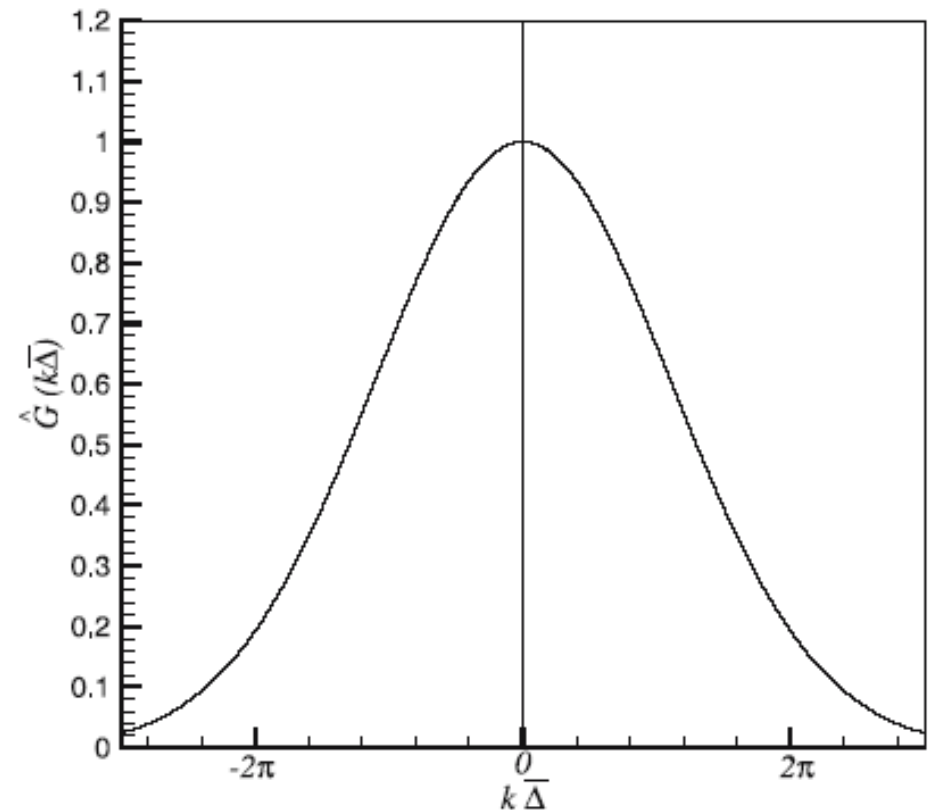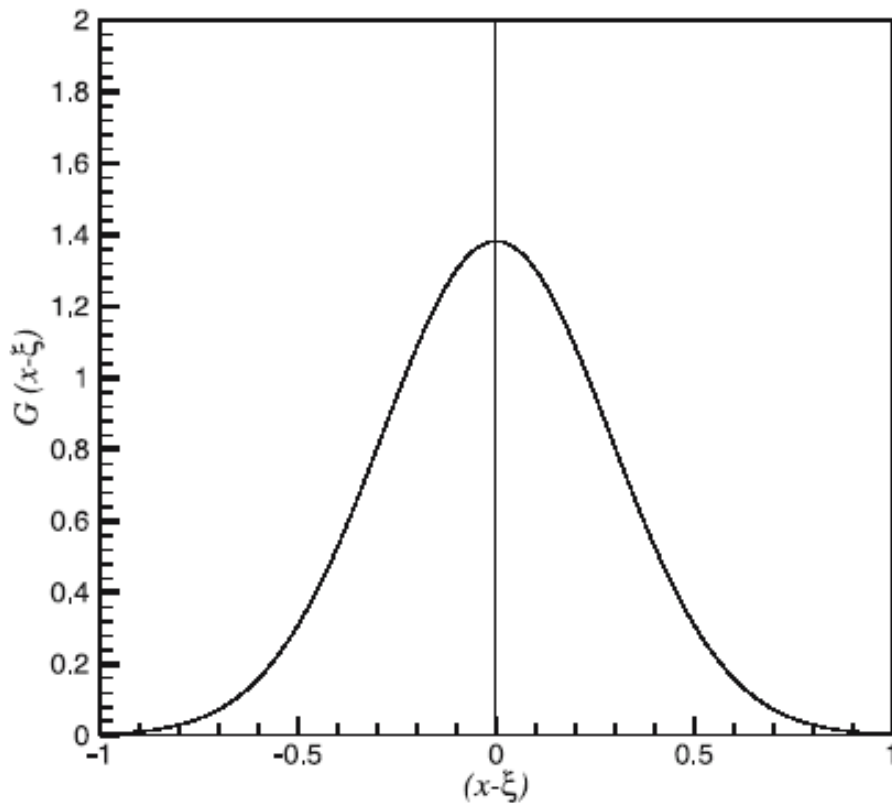
In the spectral space, $\widehat{G}(k) = \dfrac{\sin(k\overline{\Delta}/2)}{k\overline{\Delta}/2}$
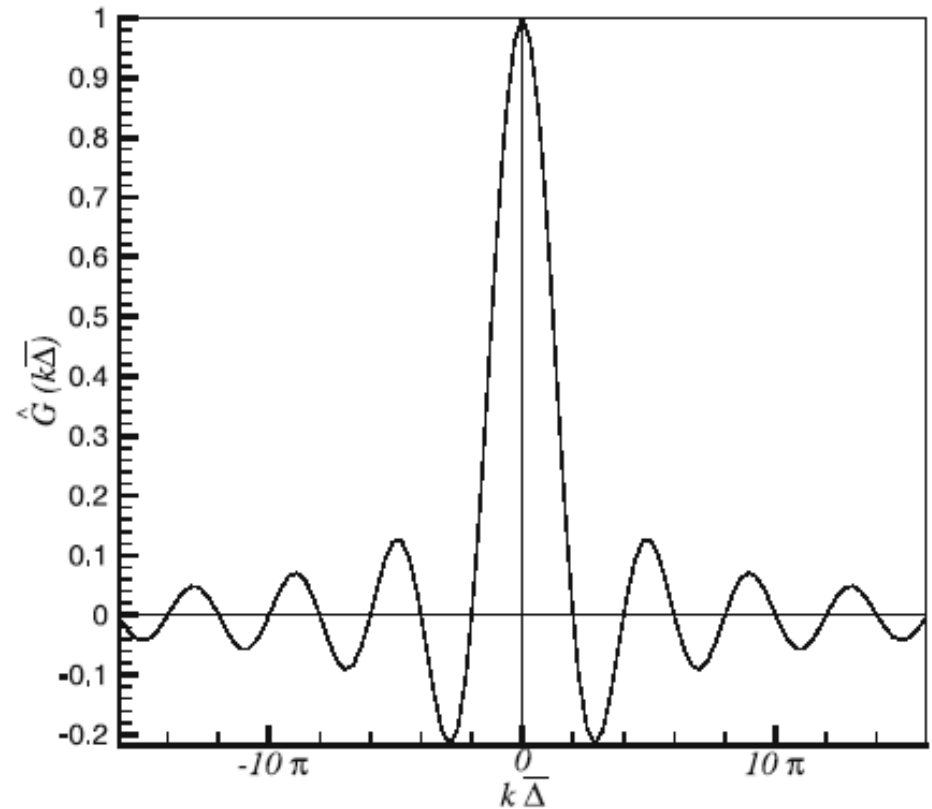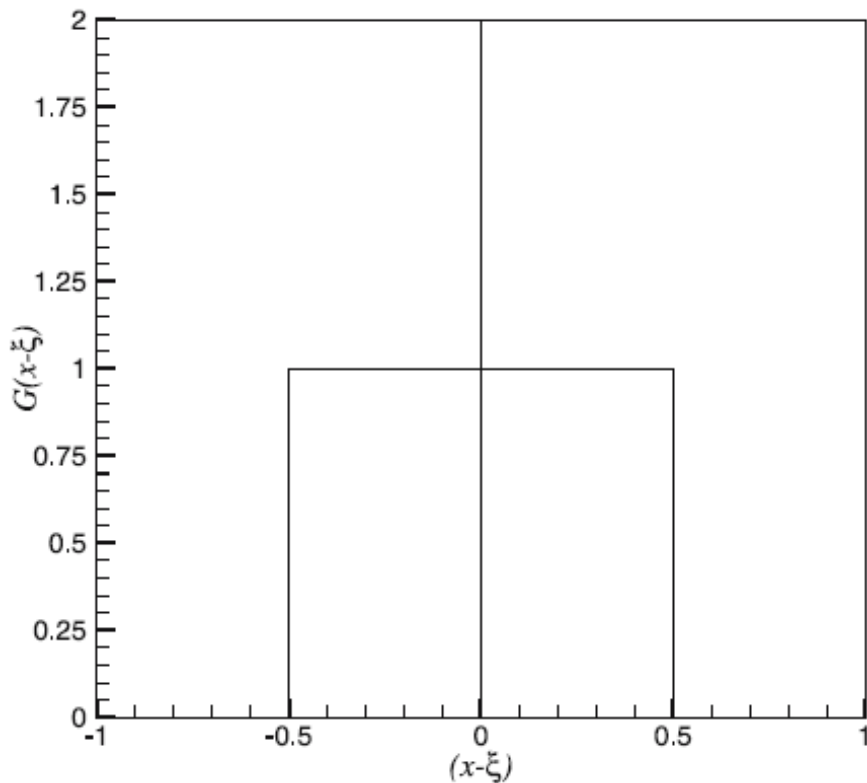
$$G(x - \xi) = \left(\frac{\gamma}{\pi \overline{\Delta}^2}\right)^{1/2} \exp\left(\frac{-\gamma |x - \xi|^2}{\overline{\Delta}^2}\right)$$

In the spectral space, $\widehat{G}(k) = \exp\left(\frac{-\overline{\Delta}^2 k^2}{4\gamma}\right)$

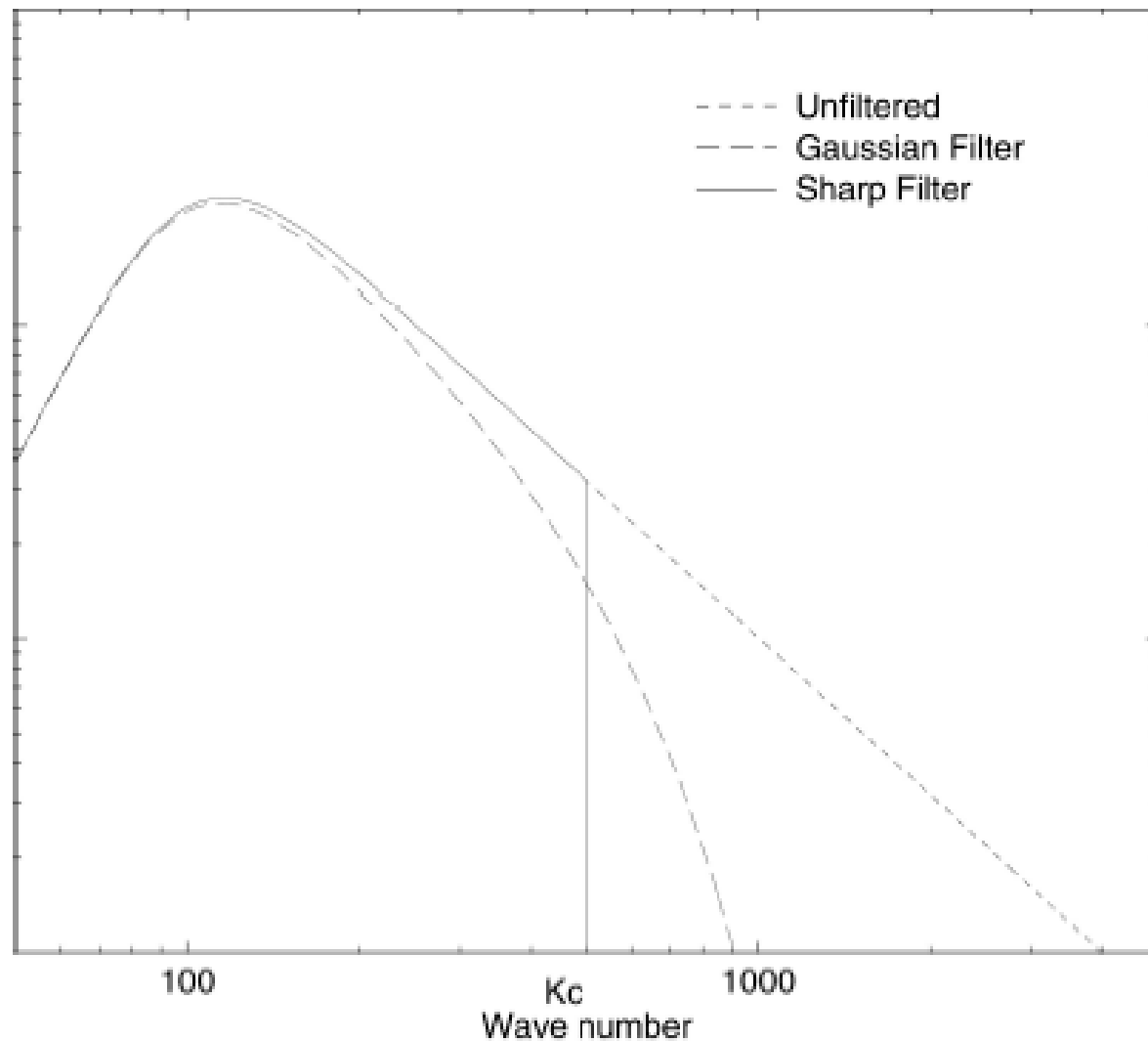in which γ is a constant generally taken to be equal to 6.

$$G(x - \xi) = \frac{\sin\left(k_c(x - \xi)\right)}{k_c(x - \xi)}, \text{ with } k_c = \frac{\pi}{\overline{\Delta}}$$

In the spectral space,
$$\widehat{G}(k) = \begin{cases} 1 & \text{if } |k| \leq k_c \\ 0 & \text{otherwise} \end{cases}$$
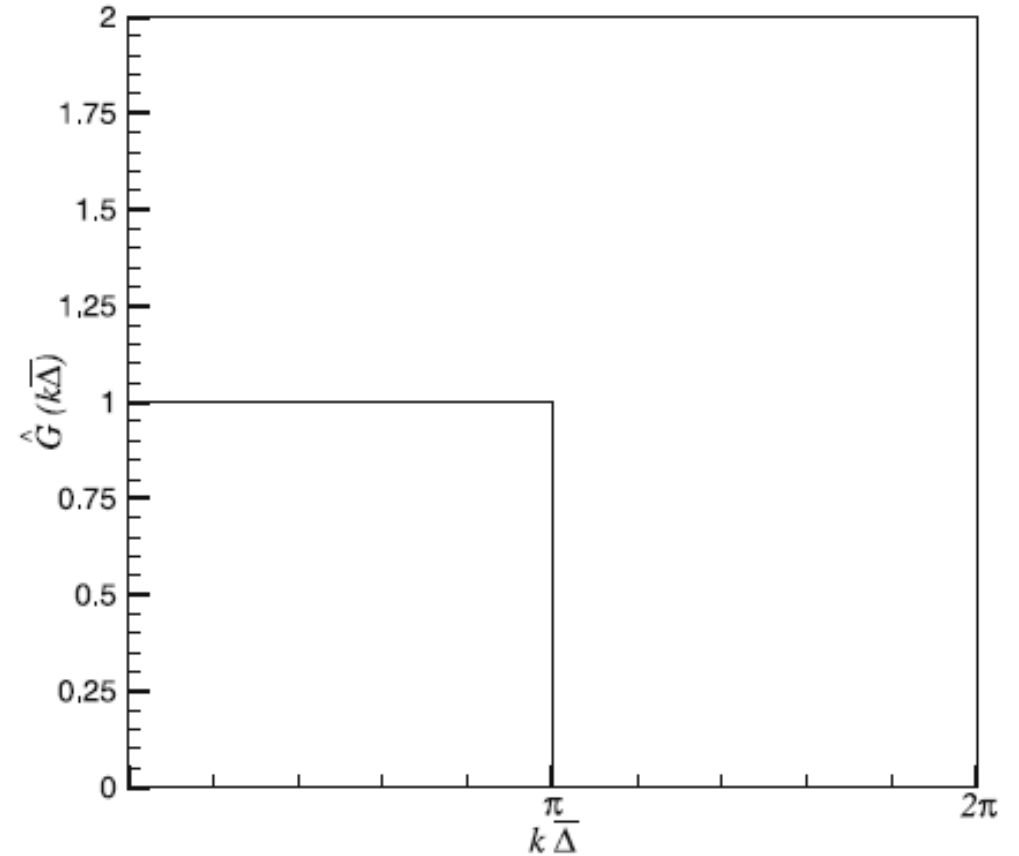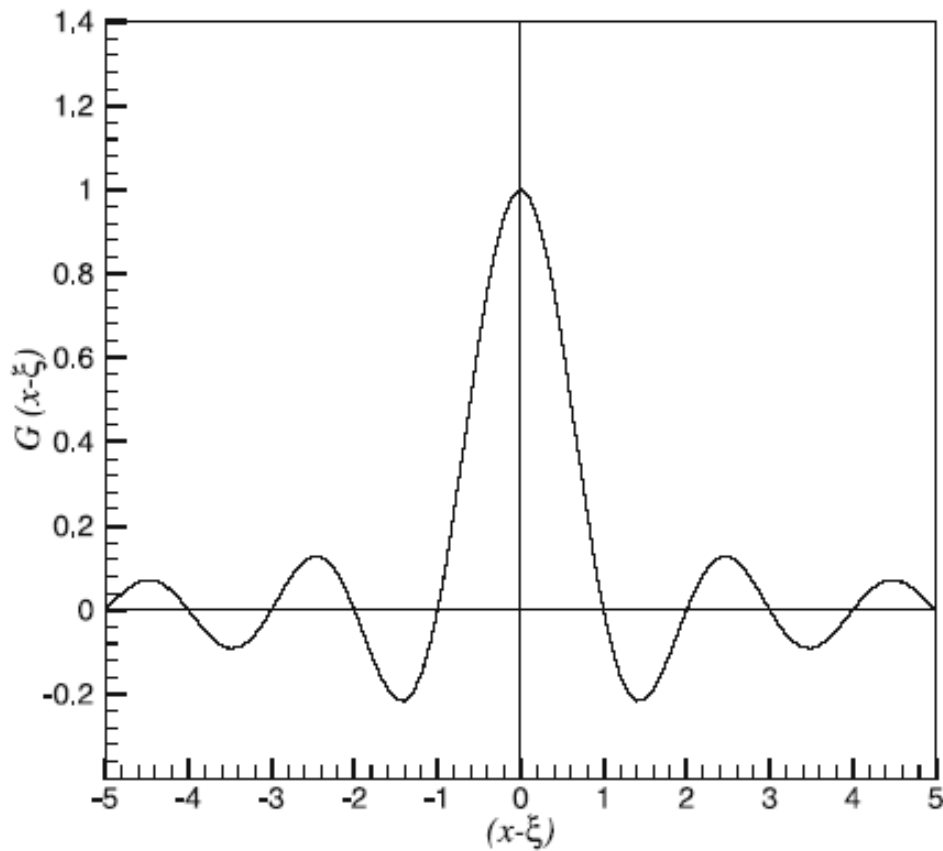
Energy spectrum of the unfiltered and filtered solutions. Filters considered are a projective filter (sharp cutoff filter) and a smooth filter (Gaussian filter) withthe same cutoff wave number $kc = 500$.